Colloid & Polymer Science Colloid Polym Sci 272:1486–1497 (1994)

Phase diagram for microphase separation transition in poor solvent polymer solutions*)

E. E. Dormidontova, I. Ya. Erukhimovich, and A. R. Khokhlov

Physics Department, Moscow State University, Moscow, Russia

*) *This paper is dedicated to Prof. E. W. Fischer on the occasion of his 65th Birthday.*

This work was done in the course of the Humboldt Research Award stay of A.R. Khokhlov at the Max-Planck-Institute for Polymer Research in Mainz. During this stay A.R.K. greatly benefited from numerous discussions with Professor E.W. Fischer who introduced him to the fascinating field of glass transition in polymer systems and formulated several new directions for future research.

Abstract: In the present paper, we consider the possibility of microphase separation transition in poor solvent polymer solutions. It is shown that this phenomenon can take place if the following two conditions are fulfilled: i) there is a large entropic contribution to the entropy of polymer/solvent mixing, i.e., solvent acts like a "plastisizer"; ii) this entropic contribution is nonlocal. Both conditions are met below the glass transition temperature for the pure polymer near the so-called Berghmans point when the glass transition curve intersects the liquid–liquid phase separation curve for polymer solutions. The phase diagram for the microphase separation transition is calculated within the framework of "weak segregation approximation" first proposed by Leibler for block-copolymer systems. The regions of stability of different microdomain structures (lamellar, triangular, body-centered-cubic) are obtained. It is shown that under certain conditions the phase diagram can have two critical points related to the macro- and microphase separation respectively.

Key words: Glass transition – microphase separation – polymer solutions

1. Introduction

Microphase separation is a widespread phenomenon in polymer physics. Investigations of microphase separation have been carried out for different polymer systems: block-copolymers [1–5], random copolymers [6–9], interpenetrating polymer networks [10–11], weakly charged polyelectrolytes in poor solvents and mixtures of weakly charged polyelectrolytes [12–19], and ionomers [20].

The specific reasons leading to the formation of the thermodynamically stable microdomain structure may be different for different systems. However, there is a common physical feature for each of the above-mentioned examples: namely, the interplay between the short-range immiscibility tendency and the opposite long-range stabilizing factor which prevents the macroscopic demixing of the polymer system. For example, this stabilizing factor may be due to connectivity of the blocks in one chain (for block copolymers, ionomers, interpenetrating networks) or due to the contribution of mobile counterions to the entropy of mixing (for polyelectrolytes).

Recently, one more polymer system exhibiting microphase separation transition has been studied [21]: polymer blends with nonlocal entropy of mixing. In ref. [21] it was shown that the balance between the short-range immiscibility

tendency caused by energetic reasons and stabilizing factor resulting from the nonlocality of entropy can lead, under certain conditions, to the formation of microdomain structure in this system. The main conditions for this effect are: i) significant negative entropic contribution to miscibility (i.e, to the Flory–Huggins parameter χ); and ii) the nonlocal character of this contribution. Both these conditions can be met for miscible polymer blend somewhat above the glass transition temperature (for the blend).

There are some experimental facts showing that this microdomain structure can indeed be formed under certain conditions for the well-known miscible blend of polystyrene (PS) and poly(vinylmethylether) (PVME) above the glass transition temperature [22–24]. For instance, the two-dimensional wideline separation NMR experiments of ref. [22] were carried out at 320 K (60 K above the glass transition temperature which is $T_g = 260$ K for 50:50 blend) and clear indication of non-heterogeneity of the characteristic size 3.5 ± 1.5 nm. was obtained. The possibility of explaining this microseparation by nonlocality of entropy has been discussed in ref. [21].

The analysis of the reasons leading to the formation of the microdomain structure in the polymer blends with nonlocal entropy of mixing [21] allows us to believe that the same reasons can lead to microphase separation in polymer solutions. Therefore, the first major aim of the present paper is to show that microphase separation can take place in poor solvent polymer solutions as well. Another aim is to calculate the full phase diagram containing not only the spinodals of macro- and microphase separation (only these curves were obtained in ref. [21]), but also the binodals which define the regions of stability of ordered (supercrystal) phases having different symmetries as well as the regions of coexistence of these phases. To do this, we will obtain not only the stability conditions for homogeneous solution, but also the characteristics of final microdomain structure.

The further consideration of this paper is organized as follows. In section 2, we present arguments qualitatively explaining the possibility of microphase separation in poor solvent polymer solutions. The free energy of the system under consideration and the stability of polymer solution with respect to macro- and microphase separation are considered in section 3. In section 4, we calculate the simplified phase diagram of the system under consideration in the weak segregation approximation proposed by Leibler [3]. Finally, in section 5 we construct the full phase diagram containing the regions of stability of different supercrystal phases (lamellar, triangular, body-centered-cubic (BCC)), as well as the regions where these phases coexist.

2. The possibility of microphase separation in poor solvent polymer solutions

As was already mentioned in the introduction, the arguments which led us in ref. [21] to the conclusion that microphase separation is possible for polymer blends apply to poor solvent polymer solutions as well. To be definite, let us consider the classical polystyrene/cyclohexane mixture. The phase diagram for this system is well known and is shown schematically in Fig. 1.

In Fig. 1, T is temperature and Φ is volume fraction of polystyrene in the solution. $\Phi = 1$ corresponds to bulk polystyrene and the glass transition temperature $T_g \approx 100\,^{\circ}\mathrm{C}$ is marked by point D. As some amount of cyclohexane is added ($\Phi < 1$) the glass transition temperature decreases

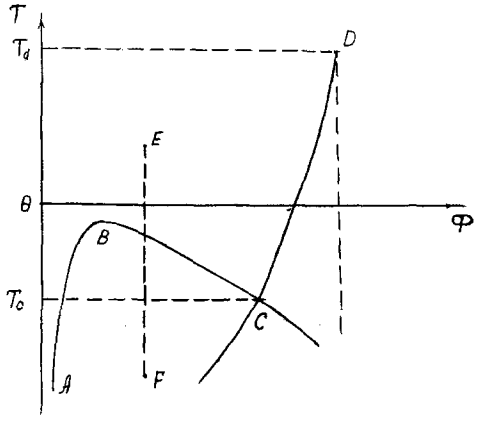

Fig. 1. Schematic phase diagram for polystyrene-cyclohexane system (T-temperature, Φ-volume fraction of polystyrene in the solution) θ-temperature corresponds to $\theta = 35\,^{\circ}\mathrm{C}$ glass transition temperature for pure polystyrene ($\Phi = 1$) is $T_g \simeq 100\,^{\circ}\mathrm{C}$. ABC-curve of liquid/liquid macroscopic phase separation (B is the critical point). DC-glass transition curve. Both curves intersect at the point C (Berghmans point)

considerably (curve DC) because solvent molecules act like "plasticizers". The point θ corresponds to the θ-temperature for polystyrene–cyclohexane system which is $\theta \approx 35\,^{\circ}C$. The curve ABC is the usual liquid–liquid macroscopic phase separation curve. The critical point B corresponds to the temperatures slightly below the θ-point. The phase separation curve intersects with the glass transition curve at the point C which is called Berghmans point [25–26].

Let us consider the poor solvent region $T < \theta$ in Fig. 1. In dilute regime $\Phi \ll 1$ the main effect is energetic inconvenience of polymer–solvent contacts which finally leads to macroscopic phase separation (curve ABC). However, at higher concentrations ($\Phi \simeq 1$), especially near the glass transition curve DC, another effect becomes important. Namely, freezing of the system at the glass transition results in the decrease of conformational entropy. Since solvent molecules act as "plasticizers", their presence prevents this entropy decrease, therefore, for entropy reasons, the polymer/solvent system tends to compatibilize, while, for energy reasons the opposite segregation tendency still exists because the solvent is poor ($T < \theta$). This entropic compatibility effect leads, in particular, to anomalously effective adsorption of gas and liquid molecules by polymers near the glass transition described recently in ref. [27].

Therefore, for the concentrated solutions of glassy polymers in poor solvents (i.e., in the vicinity of the Berghmans point C of the phase diagram of Fig. 1) there should be an effective interplay between the short range energetic repulsion and entropic compatibilizing factor. This interplay is the necessary condition for the existence of microphase separation transition (see the introduction). However, another condition must be satisfied to make microdomain structure corresponding to the true thermodynamic equilibrium. Namely, the effective spatial scale of entropic stabilizing factor should be much larger than the scale of the short-range energetic repulsion.

This latter condition is also fulfilled near the glass transition curve DC (and slightly above this curve). The reasons for this were explained in detail in ref. [21] and are connected with the nonlocality of the entropy of mixing which becomes more and more pronounced as the glass transition temperature is approached. Indeed, near the glass transition the freedom for conformational rearrangements for a given monomer unit (which defines the conformational entropy of this unit) depends not only on the closest neighbors, but on the presence of "plasticizing" molecules in the more extended surrounding. A simple illustration is shown in Fig. 2 which represents the classical game first invented by S. Loyd [28] "15 squares on 16 sites". Due to the presence of only one unoccupied site (i..e, plasticizing molecule) exactly one-half of all possible rearrangements of squares (i.e., large enough entropy) is possible [28], although to reach a given rearrangement (conformation) a complicated correlated motion of all squares is required. This is in agreement with the generally assumed fact that the approach to the glass transition temperature is accompanied by the essential increase of the size of cooperatively rearranging unit [29]. Following, ref. [21], let us denote the radius of nonlocality of the entropy of mixing as R and let us assume that in the vicinity of the Berghmans point C (the region which is of importance for us in the present paper) R is much larger than the size of a monomer unit a.

In this case, it is clear that the microdomain structure with alternating polymer-rich and solvent-rich regions of characteristic size of domains of order R corresponds to lower free energy than both homogeneous and macroscopically phase separated mixtures. Indeed, in the microdomain phase there are much less energetically unfavorable polymer-solvent contacts; on the other hand, the entropy loss is much lower than for macroscopic phase separation, because within the

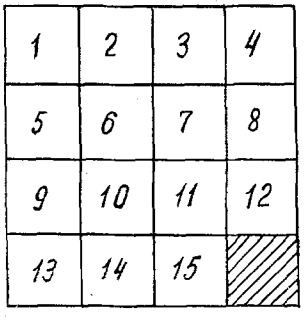

Fig. 2. Game "15 squares on 16 sites". 15 sites are filled with numbered squares, 16th site is open. The aim is to reach a given arrangement of numbered squares (e.g., shown in the figure) from the random arrangement. This can be done for exactly one half of the initial arrangements. In the case of two vacancies (i.e., 14 filled sites) all possible rearrangements (i.e., maximum possible entropy) can be reached

nonlocality radius R there are always enough "plasticizing" solvent molecules.

These qualitative arguments for the existence of the microphase separation transition in poor solvent polymer solutions in the vicinity of the Berghmans point will be confirmed in the following sections by the explicit calculation of the phase diagram.

At this point, it is worth-while to emphasize two more points.

First, we discussed the specific example of polystyrene/cyclohexane system in order to be definite. It is clear that the same effect should be observed for poor solvent solutions of any polymer which is glassy in the bulk state.

Second, the equilibrium microphase separation transition should not be mixed with the formation of frozen-in microstructures which can take place if the solution is rapidly quenched from the good solvent conditions to the temperatures below the Berghmans point temperature T_c (e.g., along the line EF in Fig. 1). In the latter case the spinodal decomposition process will be kinetically stopped because of the glass transition in the polymer-rich regions. The emerging frozen-in microstructures has been studied experimentally (see, e.g., ref. [26]) and are known to be dependent on the specific type of the quenching process (one-step quenching, two-step quenching etc.; see ref. [26]). At the same time, the microdomain structures discussed above correspond to the region above the glass transition curve CD and to thermodynamic equilibrium, i.e., they depend only on the point on the (T, Φ)-diagram, but not on the previous history of the process.

In this section the qualitative arguments to explain the possibility of microphase separation in poor solvent polymer solutions were presented. In the next sections we investigate quantitatively the conditions for microphase separation transition, construct the full phase diagram, and calculate the properties of the emerging micro-domain structure.

3. The stability of the polymer solution with nonlocal entropy of mixing with respect to microphase separation and free energies of the ordered phases

Let us consider the solution of flexible polymer chains, each consisting of N monomer units. For the physical situation qualitatively discussed in the previous section the free energy of the solution can be written in the form:

$$F = F_1 + F_e \,, \tag{1}$$

where F_1 is the ordinary free energy and F_e is the specific contribution associated with nonlocal entropy of mixing.

To describe the interactions in polymer solution we will use the Flory–Huggins lattice model with the size b of an elementary cell and the Flory–Huggins parameter of direct energetic interactions between monomer units χ_e. The chains are assumed to be flexible, therefore their Kuhn segment length a is of order b.

Within the framework of self-consistent field approximation the free energy of the solution F_1 with inhomogeneous distribution of polymer concentration can be written in the following form:

$$\frac{F_1}{kT} = \int \frac{dV}{b^3} \left\{ \frac{\Phi}{N} \ln \Phi + (1 - \Phi) \ln (1 - \Phi) + \chi_e \Phi (1 - \Phi) + \frac{a^2}{24} \frac{(\nabla \Phi)^2}{\Phi} \right\}, \tag{2}$$

where $\Phi(r)$ is the volume fraction of polymer at the point r.

The first two terms of the expression (2) correspond to the translational entropy of polymer chains and solvent molecules respectively. The third term describes the short-range polymer–solvent interaction. The last term corresponds to so-called Lifshitz entropy [30–32], i.e., the nonlinear entropy loss resulting from inhomogeneous distribution of polymer concentration. Even though the more exact expression for the last term of the free energy can be written in terms of response functions in the expansion of the free energy [3], the form (2) is equivalent to it asymptotically if the characteristic scale $L = 2\pi/q$ of the inhomogeneities occurring in the system is much smaller than the macromolecular size R (i.e., in the limit $x = a^2 q^2 N/6 \gg 1$). As can be seen from the results (see below) this inequality is generally valid for the system under investigation. Thus, the form (2) for the free energy is quite sufficient for our purposes.

The contribution F_s to the free energy (2) related to the non-local entropy of mixing can be

represented as follows [21]:

$$\frac{F_s}{kT} = \frac{F_{s0}}{kT} + \frac{1}{b^3}\int \Phi(r)\Delta S(r-r')\Phi(r')\,dV\,dV'/2\,, \tag{3}$$

where the kernel $\Delta S(r-r')$ is a positive function of its argument tending to zero at $|r-r'| \Rightarrow \infty$. The derivation of Eq. (3) is completely analogous to that of ref. [21], so we do not repeat it here. Then the integral magnitude of the effect S and the nonlocality radius R (see section 2) can be defined as follows:

$$S = \frac{1}{b^3}\int \Delta S(r-r')\,dV' \tag{4}$$

$$R = \frac{\int |r-r'|^2 \Delta S(r-r')\,dV'}{\int \Delta S(r-r')\,dV'} \tag{5}$$

As in ref. [21], it is easy to show that S is the entropic contribution to the Flory–Huggins parameter, i.e., the effective value of this parameter is

$$\chi = \chi_e + \chi_s = \varepsilon/kT - S \tag{6}$$

As regards the exact form of the function $\Delta S(r-r')$, it can be defined from the detailed microscopic considerations only, but its general features can be guessed from the simple physical arguments. We can assume that it should be rapidly decreasing function, because for $r \gg R$ the influence of surrounding links becomes negligible. From the analogy with the theory of phase transitions ([33]) we can suggest for $\Delta S(r-r')$ the following form (cf. ref. [21]):

$$\Delta S(r-r') = \frac{3S}{2\pi R^2}\,\frac{\exp(-\sqrt{6}|r-r'|/R)}{|r-r'|} \tag{7}$$

Using the expression (7) for $\Delta S(r-r')$, we can completely define (in terms of the parameters S and R) the contribution F_s (3) to the free energy of polymer solution, associated with the nonlocal entropy.

Let us consider small deviations of function $\Phi(r)$ from the average value $\langle\Phi\rangle$: $\tilde{\Phi}(r) = \Phi(r) - \langle\Phi\rangle$; $|\tilde{\Phi}(r)| \ll \langle\Phi\rangle$. Then the expansion of the free energy F in the powers of these deviations $\tilde{\Phi}(r)$ can be written (after the Fourier transformation) in the following conventional form [3]:

$$\frac{F}{kT} = \frac{F_0}{kT} + \frac{1}{b^3}\sum_{n=2}^{4}\frac{1}{n!}(\Gamma^{(n)}\tilde{\Phi}^{(n)})\,, \tag{8}$$

where the notation

$$(\Gamma^{(n)}\tilde{\Phi}^{(n)}) = \int \Gamma^{(n)}(q_1, \ldots, q_n)\prod_{i=1}\tilde{\Phi}(q_i)\frac{d^n q_i}{(2\pi)^3}$$

is introduced. Thereby the kernels $\Gamma^{(n)}(q_1, \ldots, q_n)$ are defined explicitly as follows (cf. ref. [21]):

$$\Gamma^{(n)}(q_1, \ldots, q_n) = (2\pi)^3\tilde{\Gamma}^{(n)}(q_1, \ldots, q_n)\delta\left(\sum_{i=1}^{n} q_i\right)$$

$$\tilde{\Gamma}^{(2)}(q) = \frac{1}{(1-\langle\Phi\rangle)} - 2\chi_e + \Delta S(q) + \frac{a^2q^2}{12\langle\Phi\rangle}$$

$$\tilde{\Gamma}^{(3)}(q_1, q_2, q_3) = \frac{1}{(1-\langle\Phi\rangle)^2} - \frac{a^2(q_1^2+q_2^2+q_3^2)}{24\langle\Phi\rangle^2};$$

$$\tilde{\Gamma}^{(4)}(q_1, q_2, q_3, q_4) = \frac{2}{(1-\langle\Phi\rangle)^3} + \frac{a^2}{12\langle\Phi\rangle^3}(q_1^2 + q_2^2 + q_3^2 + q_4^2)\,. \tag{9}$$

In Eq. (9)

$$\Delta S(q) = \frac{S}{1 + q^2R^2/6} \tag{10}$$

is the Fourier transformation of the function $\Delta S(r)$ defined by Eq. (7). In Eq. (8) F_0 is the free energy of the homogeneous (disordered) phase:

$$\frac{F_0}{kT} = \frac{V}{b^3}\left\{\frac{\langle\Phi\rangle}{N}\ln\langle\Phi\rangle + (1-\langle\Phi\rangle)\ln(1-\langle\Phi\rangle) + \chi\langle\Phi\rangle(1-\langle\Phi\rangle)\right\} \tag{11}$$

First, let us analyze the stability of homogeneous state of the solution. For this purpose the second order term of the free energy expansion (8) should be considered in more detail.

The spinodal equation for microphase separation (i.e., the boundary of stability of a homogeneous state with respect to microphase separation) can be found from the conditions ([3, 4]):

$$\begin{cases}\left(\dfrac{d\tilde{\Gamma}^{(2)}(q)}{dq}\right)_{T\phi} = 0\\ \tilde{\Gamma}^{(2)}(q) = 0;\end{cases} \tag{12}$$

Solving Eq. (12), we get the expressions for critical vector q^* as well as for the critical value of Flory–Huggins parameter χ_{cr} (it should be remembered that $\chi = \chi_e - S$) corresponding to

spinodal of microphase separation:

$$a^2 q_*^2 = 6S(2\sqrt{\langle\Phi\rangle/\Sigma} - 1/\Sigma) \tag{13}$$

$$2\chi_{cr} = \frac{1}{1-\langle\Phi\rangle} - 2S + \frac{2S}{\sqrt{\Sigma\langle\Phi\rangle}} - \frac{S}{2\Sigma\langle\Phi\rangle}. \tag{14}$$

The parameter $\Sigma = SR^2/a^2$ in Eqs. (12) and (13) depends on both characteristics of the nonlocal entropy effect: its integral magnitude S and the nonlocality radius R.

In order to make sure that we have a microphase (rather than macrophase) separation the unequality

$$q_*^2 \geq 0 \tag{15}$$

should be fulfilled. This inequality (15) results in the following condition supplementing Eqs. (13) and (14):

$$\Phi > \Phi_{bound} = \frac{1}{4\Sigma}. \tag{16}$$

In Fig. 3 the spinodal curves for microphase (dashed lines) and macrophase (solid line) separation are shown for $N = 10^3$, $S = 1$ and different values of Σ. As can be seen from Fig. 3, the region of microphase separation (which is situated between the solid and the corresponding dashed line) is getting larger with the increase of Σ, i.e., with the increase of the nonlocality radius R.

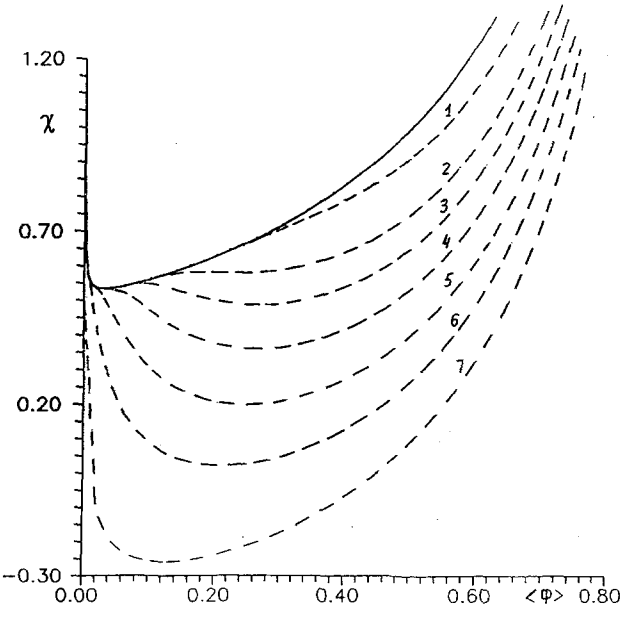

Fig. 3. Spinodal curves for the polymer solution for $N = 10^3$, $S = 1$. The dashed curves 1–7 correspond to spinodals for microphase separation for $\Sigma = 1, 2, 3, 5, 10, 25, 250$ respectively, the solid curve is the one for macrophase separation

In Figs. 4 and 5 the values of $q_*^2 a^2$ and $D/a \equiv 2\pi/q^* a$ respectively are plotted as functions of $\langle\Phi\rangle$ for the same set of parameters as in Fig. 3. It follows from Eqs. (13) and (16) that the value of q_* normally increases (and hence the period of D decreases) with the increase of Σ (i.e., with the increase of the nonlocality radius R associated with the influence of the chain surrounding). One can see that the period of microdomain structure $D = 2\pi/q^*$ is normally (not too close to Φ_{bound}) of the order of several times of a ($D/a \approx 5$–10) which is considerably smaller than the macromolecular size $R_a = aN^{1/2}$ and corresponds to non-heterogeneity. Note, however, that $q_* \Rightarrow 0$ and $D \Rightarrow \infty$ when $\Phi \Rightarrow \Phi_{bound}$. Hence, a rather larger-scale microstructure can emerge for this case.

Now, let us rewrite the expansion (8) for the free energy in the following form (cf. ref. [3, 19]):

$$\frac{F}{kT} = \frac{F_0}{kT} + (\chi - \chi_{cr})\sum_q \tilde{\Phi}(q)\tilde{\Phi}(-q) + \frac{1}{6}S_3 \sum_{q_1+q_2+q_3} \tilde{\Phi}(q_1)\tilde{\Phi}(q_2)\tilde{\Phi}(q_3) + \frac{1}{24}S_4 \sum_{q_1+q_2+q_3+q_4} \tilde{\Phi}(q_1)\tilde{\Phi}(q_2)\tilde{\Phi}(q_3)\tilde{\Phi}(q_4), \tag{17}$$

where

$$S_3 = \frac{1}{(1-\langle\Phi\rangle)^2} - \frac{a^2 q_*^2}{8\langle\Phi\rangle^2}; \tag{18}$$

$$S_4 = \frac{2}{(1-\langle\Phi\rangle)^3} - \frac{a^2 q_*^2}{3\langle\Phi\rangle^3}. \tag{19}$$

Or, we can write

$$\frac{F}{kT} = \frac{F_0}{kT} + 2(\chi_{cr} - \chi)\Phi_n^2 + \alpha_n \Phi_n^3 + \beta_n \Phi_n^2, \tag{20}$$

where Φ_n is the equilibrium value of the amplitude of the order parameter which should be obtained by minimizing the expression (18) with respect to Φ_n, the quantity χ_{cr} is defined by expression (14), and α_n, β_n are the coefficients which take the

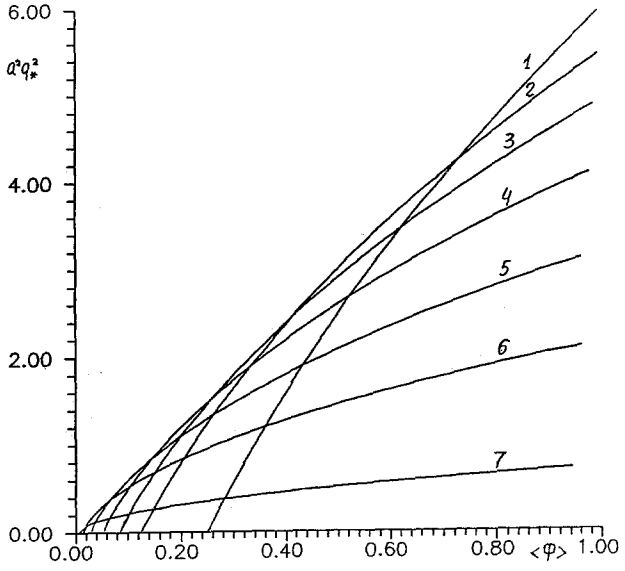

Fig. 4. The plots of the critical wave vector $q_*^2 a^2$ as functions of the average value of volume fraction of polymer $\langle \Phi \rangle$ related to the curves 1–7 of Fig. 3 ($S = 1$)

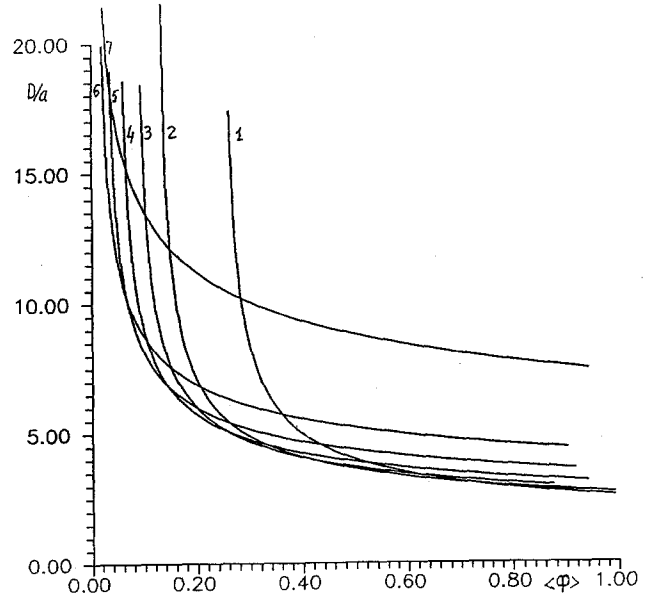

Fig. 5. The plots of the period of microstructure D/a as functions of average value of volume fraction of polymer $\langle \Phi \rangle$ related to the curves 1–7 of Fig. 3 ($S = 1$)

following form for conventional lattices [3]:

$$\text{for lamellar lattice} \quad \alpha_1 = 0, \quad \beta_1 = \frac{1}{4} S_4 ,$$

$$\text{for triangular lattice} \quad \alpha_3 = \frac{2}{3(3)^{1/2}} S_3, \quad \beta_3 = \frac{5}{12} S_4 , \tag{21}$$

$$\text{for body-centered-cubic lattice} \quad \alpha_6 = \frac{4S_3}{3(6)^{1/2}}, \quad \beta_6 = \frac{5}{8} S_4 .$$

Minimizing the free energy (18) with respect to Φ_n, we obtain the following expressions for the free energy of different microdomain structures:

for lamellar (LAM) structure ($n = 1$):

$$\frac{F_1}{kT} = \frac{F_0}{kT} - \frac{(\chi - \chi_{cr})^2}{\beta_1} , \tag{22}$$

for the triangular (Δ) and body-centered-cubic (BCC) structures ($n = 3$ and $n = 6$ respectively)

$$\frac{F_n}{kT} = \frac{F_0}{kT} + \frac{27\alpha n^4}{(64)^2 \beta_n^3} (1 + \gamma_n)^3 (1 - 3\gamma_n) , \tag{23}$$

where

$$\gamma_n = \left(1 + \frac{64 \beta_n (\chi - \chi_{cr})}{9 \alpha_n^2} \right)^{1/2} . \tag{24}$$

4. A simplified phase diagram

The analysis given in the previous section enables us to compare numerically the free energies of the ordered phases (22)–(23) and of the homogeneous one (10) and determine in this way the regions where the homogeneous (disordered) phase (DIS) or a given ordered one has the lowest free energy at given average value of the polymer volume fraction $\langle \Phi \rangle$. We will call the corresponding diagram (in the variables $\langle \Phi \rangle$ and χ) the simplified phase diagram. The conventional phase diagram taking into account the possibility of further decrease of the full free energy of the system by allowing its macroscopic separation into two coexisting phase having different values of $\langle \Phi \rangle$ will be constructed in the next section

It is worthwhile to emphasize here that, for the case of microphase separation in the melt of block-copolymers, the simplified phase diagram

coincides with the conventional one, because the macroscopic phase separation is impossible. On the simplified phase diagram the line of the transition DIS-BCC is determined by (cf. ref. [3])

$$\chi_{06} = \chi_{cr} - \frac{\alpha_6^2}{8\beta_6} . \tag{25}$$

The line of the transition LAM-Δ is:

$$\chi_{13} = \chi_{cr} + \frac{9\alpha_3^2(\gamma_3'^2 - 1)}{64\beta_3} , \tag{26}$$

where $\gamma_3' = 3 + 6^{1/2}$. Finally, the line of the transition Δ-BCC can be determined by the solution of

$$F_6 = F_3 , \tag{27}$$

the functions F_n being defined by Eq. (23).

Before explicitly constructing the simplified phase diagrams, let us first locate the critical points (if any) related to microphase separation (MPSCP). The location of MPSCP is determined by vanishing of the coefficient S_3 on the microphase spinodal (14). It should be remembered that the region of validity of the weak segregation limit is being restricted to the vicinity of the critical point [17, 34]. Substituting into the equation

$$S_3 = 0 , \tag{28}$$

the expression (19) for S_3 and expression (13) for q_*^2 we get

$$\frac{8\langle\Phi\rangle^2}{(1-\langle\Phi\rangle)^2} = 6S(2\sqrt{\langle\Phi\rangle/\Sigma} - 1/\Sigma) . \tag{29}$$

One can readily see that Eq. (29) has two or no solution with respect to $\langle\Phi\rangle$, depending on the values of parameters S and Σ (or $\rho = R/a$). The corresponding diagram of possible regimes is shown in Fig. 6. The system has two critical points if it is characterized by the values of S and ρ above the solid line and no critical points otherwise. Besides, in Fig. 6 the dashed line satisfying the equation $\Phi_{bound} = 1$ is shown. If the system belongs to the region below the dashed line on microphase separation can occur. One should stress that apart from MPSCP defined by Eq. (29) there might exist another critical point related to the ordinary macroscopic liquid–liquid phase separation of the solution.

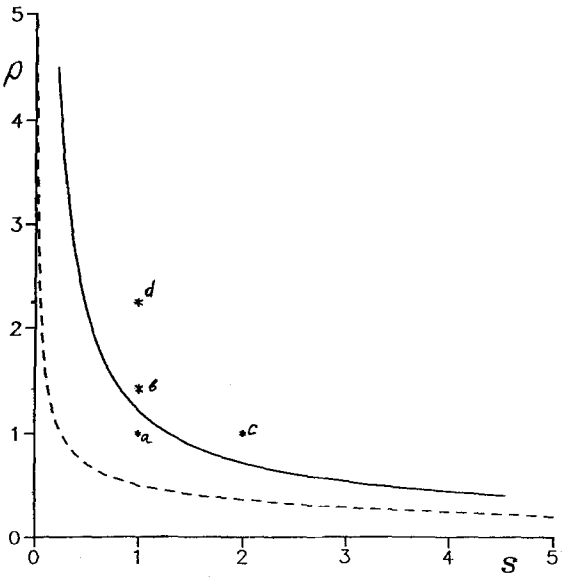

Fig. 6. The diagram of possible regimes of the behavior of the solution in the variables $\rho = R/a$ and S. The solid line separates the region, where the equation $S_3 = 0$ has two solutions (two critical points) and the region where the equation $S_3 = 0$ has no solution (below the line). The dotted line corresponds to the condition $\Phi_{bound} = 1$. The parameters, for which phase diagrams are calculated below are shown by the asterisks

One can expect that the specific features related to the presence of non-local entropy of the system will be the more pronounced at high values of the parameters S and ρ. Indeed, let us consider the simplified phase diagram calculated using Eqs. (25–27) for the values of these parameters characterized by points $a = (1, 1)$, $b = (1, \sqrt{2})$ and $c = (2, 1)$ in Fig. 6. These diagrams are shown in Figs. 7–9. In these diagrams the regions where homogeneous (DIS), BCC, triangular and lamellar phases have the lowest free energy (as compared to other homogeneous phases) are indicated.

We see that the simplified phase diagrams for the present case differ very much from the conventional phase diagrams calculated for molten block-copolymers of various architecture in refs. [3, 35, 36]. Namely, for block-copolymer phase diagrams exactly one critical point is present, whereas the simplified phase diagrams for the present cases b and c contain three critical points including one for macroscopic phase separation, and only for the case a does the single critical point remains.

Another interesting feature of the simplified phase diagrams of Figs. 7–9 is the presence of the vertical phase transition line $\Phi = \Phi_{\text{bound}}$. At high enough values of χ this is the boundary line between the regions of the disordered and ordered phases. One should note, however, that this line is, to some extent, an artifact of our procedure of comparing free energies of different phases at the same average value of Φ. The case is that, above the dashed line (the spinodal of the disordered phase), the homogeneous disordered state itself is unstable with respect to macrophase separation and, therefore, thermodynamically unfavorable. Moreover, the homogeneous state is thermodynamically disadvantageous (even though it stays metastable) even below the spinodal, but above binodal with respect to macrophase separation. In particular, for the point *a* (its simplified diagram is shown in Fig. 7) the whole region of the existence of microdomain phases is situated above the binodal where macrophase separation of the disordered phase lowers the free energy. For other situations this may be not the case, however, then

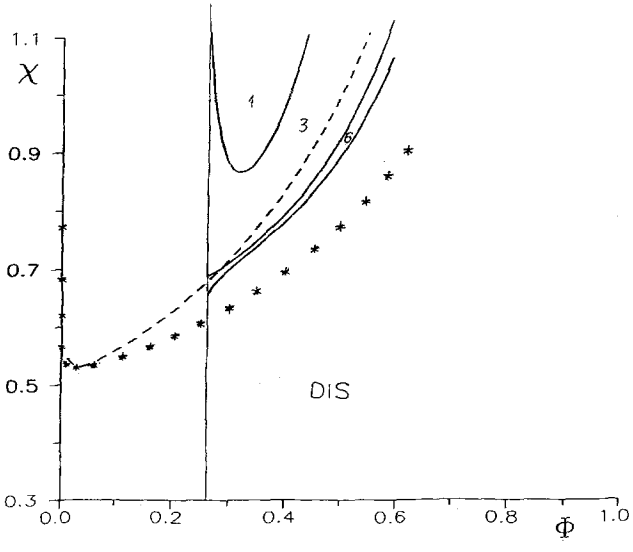

Fig. 7. Simplified phase diagram for the polymer solution with nonlocal entropy of mixing for $N = 10^3$, $S = 1$, $\rho = 1$ ($\Sigma = 1$). The regions where one of the phases has the lowest free energy are shown: the region of disordered phase (DIS), body-centered-cubic microdomain phase (6), triangular microdomain phase (3), lamellar microdomain phase (1). The dotted curve is the spinodal for macrophase separation. The asterisk curve corresponds to the binodal of macrophase separation. Vertical line is the line $\langle\Phi\rangle = \Phi_{\text{bound}}$

it is necessary to take into account the complications due to fluctuation effects which can be shown to be of great significance near the line $\Phi = \Phi_{\text{bound}}$. Thus, in what follows we restrict ourselves to the study of the systems having no observable singularity at $\Phi = \Phi_{\text{bound}}$ and exemplified by points *a*, *b* and *c*.

5. The stability of the ordered phases of the poor solvent polymer solution with nonlocal entropy of mixing with respect to macrophase separation and the complete phase diagram

Thus, in order to give a more correct description of our system, we have to take into account the possibility of macroscopic separation with the formation of different phases. To this end, one should solve the set of equation of phase equilibrium for all possible couples of phases:

$$\begin{cases} P_n = P_m \\ \mu_n = \mu_m \,, \end{cases} \tag{30}$$

where μ_k and P_k are the chemical potential $\mu = (\partial F/\partial\Phi)_{V,T}$ and the osmotic pressure $P = (\Phi\,\partial F/\partial\Phi - F)$ for the phase (for the disordered phase $k = 0$, for LAM, Δ and BCC microdomain phase $k = 1$, 3 and 6, correspondingly; cf. Eqs. (21)–(23)).

One should note that the stability of an ordered phase with respect to macroscopic phase separation is determined, as well as for the disordered phase, by the condition

$$(\partial\mu_k/\partial\Phi)_T > 0 \,. \tag{31}$$

The existence of the condition (31) is a very important difference of the systems able to undergo macroscopic phase separation from the block-copolymer-type systems with fixed value of Φ considered in refs. [3], [34]–[36]. Indeed, one can show straightforwardly that the condition (31) is not fulfilled for all ordered phases when the nonlocal entropy contribution is small enough. All the phases are unstable and the phase diagram of the system is just an ordinary phase diagram for the corresponding polymer solution. Thus, there is no non-local entropy influence on the phase behaviour of the system for this case.

However, the effect becomes observable with the increase of the parameters S and R characterizing non-local entropy. From the quantitative

solution of the set of Eqs. (30) for each pair of phases, we obtain the full phase diagrams of Figs. 10–12 for the same values of parameters as for Figs. 8 and 9 (corresponding to points *b* and *c* on Fig. 6) and also for $S = 1$, $\Sigma = 5$ (point d in Fig. 6). All phase diagrams are plotted in the variables (χ, Φ). These phase diagrams (Figs. 10–12) contain the regions of stability of different phases: disordered (DIS), BCC (6), triangular (3), lamellar (1) phases, as well as the regions of macroscopic phase separation between different phases. For relatively large values of χ only lamellar microphase survives and, also, there are broad biphasic regions of the coexistence of lamellar and homogeneous phases. The regions of stability of microdomain structure for $S = 2$, $\Sigma = 2$ (Fig. 11) and $S = 1$, $\Sigma = 5$ (Fig. 12) are wider than for $S = 1$, $\Sigma = 2$ and the phase separation appears for smaller values of χ.

The full phase diagrams for $S = 1$, $\Sigma = 2$ (Fig. 10) as well as the diagram of Fig. 11 ($S = 2$, $\Sigma = 2$) have two critical points. One of these critical points is related to the macroscopic phase separation, another one is associated with microphase separation. The presence of these two critical points has a rather important influence on the general outlook of the full phase diagram. For the values of Σ corresponding to Figs. 10 and 11 these

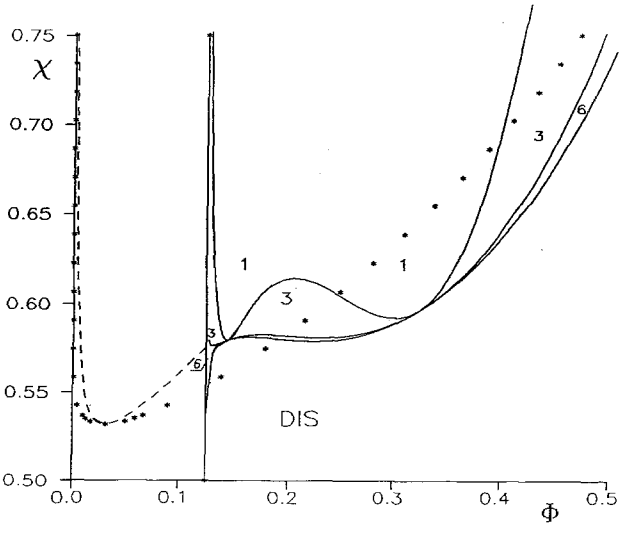

Fig. 8. Simplified phase diagram for the polymer solution for $N = 10^3$, $S = 1$, $\rho = 2^{1/2}$, ($\Sigma = 2$). The notation for different regions of the phase diagram and different curves is the same as in Fig. 7

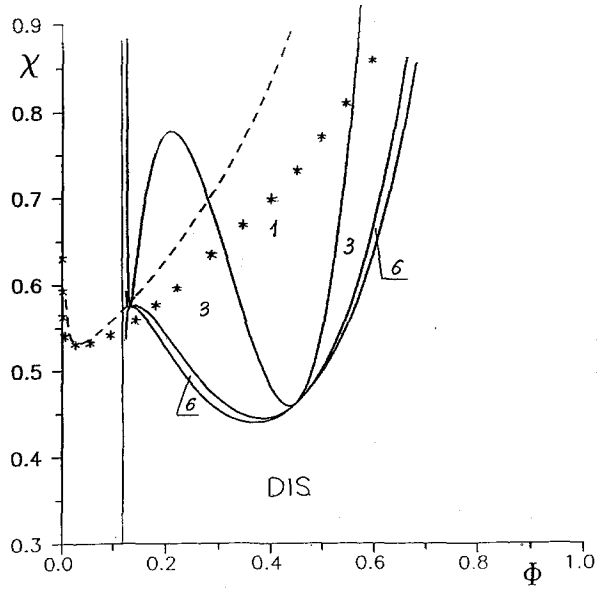

Fig. 9. Simplified phase diagram for the polymer solution for $S = 2$, $\rho = 1$, ($\Sigma = 2$). The notation for different regions of the phase diagram and different curves is the same as in Fig. 7

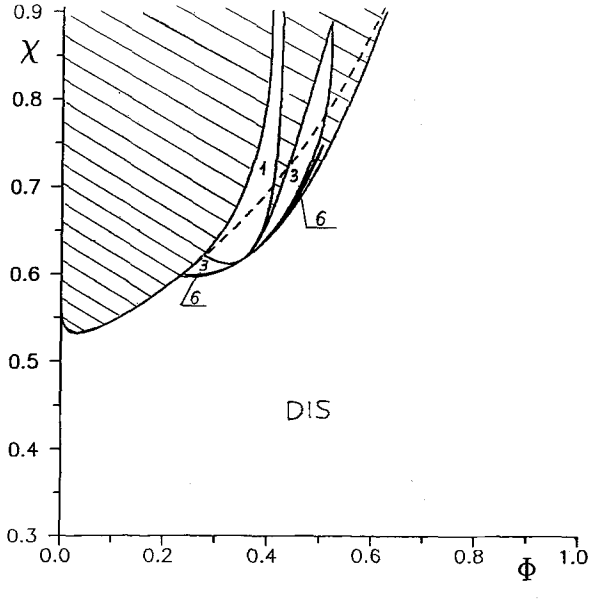

Fig. 10. Phase diagram for the polymer solution for $N = 10^3$, $S = 1$, $\Sigma = 2$. Phase diagram contains the following regions: disordered phase (DIS), body-centered-cubic microdomain phase (6), triangular microdomain phase (3), lamellar microdomain phase region (1) and the regions of phase separation (shaded regions). The dotted curve is the binodal for macroscopic phase separation

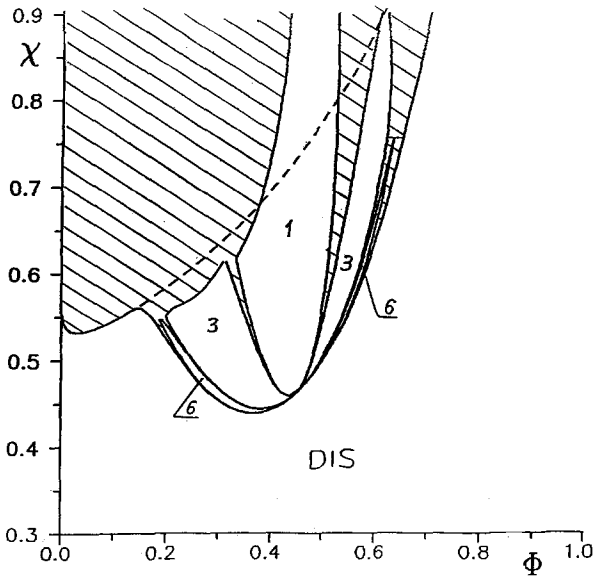

Fig. 11. Phase diagram for the polymer solution for $N = 10^3$, $S = 1$, $\Sigma = 5$. The notation is the same as in Fig. 10. The dotted curve is the binodal for macroscopic phase separation

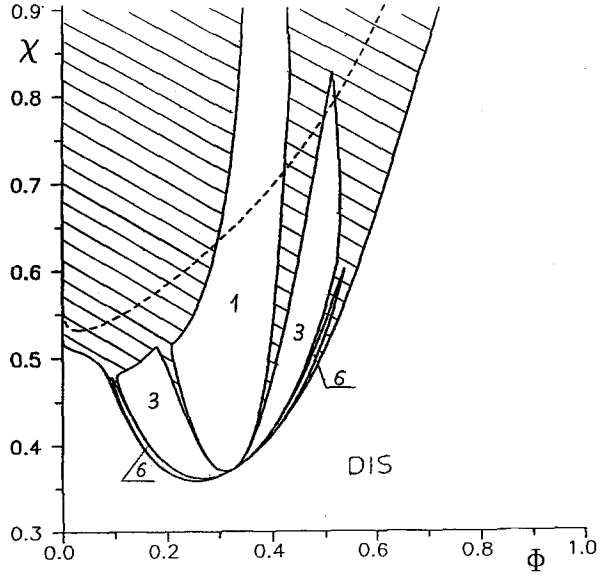

Fig. 12. Phase diagram for the polymer solution for $S = 2$, $\Sigma = 2$. The notation is the same as in Fig. 10. The dotted curve is the binodal for macroscopic phase separation

points are essentially distant from each other. With the increase of Σ the influence of the critical point related to macroscopic phase separation become smaller and for large values of Σ this critical point disappears (e.g., for $S = 1$, $\Sigma = 5$ (Fig. 12)).

The phase diagrams containing two critical points are frequently observed experimentally [37]. We can suspect that one of the possible reasons for this may be the interplay between microphase and macrophase separation. A more detailed investigation of the systems exhibiting two critical points is needed to clarify this question.

In the present paper, we have studied the polymer solutions within the framework of weak segregation approximation and, thus, our results are valid only for the region not far from the critical point. However, from the phase diagrams of Figs. 10–12 it is possible to notice that the regions of stability of different microphases correspond to the parts of the phase diagrams near the critical point, with the exception of the lamellar phase region, which also spreads far from the critical point. To obtain information about the behavior of the polymer solutions far from the critical point it is necessary to carry out a similar investigation in the strong segregation regime.

Acknowledgements

The authors are grateful to the Russian Foundation for Fundamental Research for financial support.

References

1. Developments in Block Copolymers (1982 Vol. 1), (1985 Vol. 2): Goodman I (ed) Applied Science, New York.
2. Helfand E (1975) Macromolecules 8:552
3. Leibler L (1980) Macromolecules 13:1602
4. Erukhimovich I Ya (1982) Vysokomol soedin Ser A 24, 1942, 1950 ((1983) Translated in Polymer Sci USSR 24:2223)
5. Semenov AN (1985) Sov Phys JETP 61:733
6. Shakhnovich EI, Gutin AM (1989) J de Phys (P) 50:1843
7. Panukov SV, Kuchanov SI (1991) Zh Exsp Teor Fiz (Sov Phys JETP) 99:659
8. Dobrynin AV, Erukhimovich I Ya (1991) JETP Letters 53:570
9. Fredrickson GH, Milner ST (1991) Phys Rev Lett 67:835
10. Binder K, Frisch H (1984) J Chem Phys 81:2126
11. Frisch H, Grosberg A Yu (1993) Macromol Chem Theory Simul 2:517
12. Borue V Yu, Erukhimovich I Ya (1986) Sov Phys Doklady 31:146
13. Borue V Yu, Erukhimovich I Ya (1988) Macromolecules 21:3240
14. Joanny JF, Leibler L (1990) J Physique 51:545

15. Nyrkova IA, Khokhlov AR, Kramarenko E Yu (1990) Vysokomol soedin ser A 32:918 ((1990) Polymer Sci USSR 32:852)
16. Khokhlov AR, Nyrkova IA (1992) Macromolecules 25:1493
17. Dobrynin AV, Erukhimovich I Ya (1991) Zh Eksp Teor Fiz 99:1344 ((1991) Sov Phys JEPT 72:751)
18. Nyrkova IA, Doi M, Khokhlov AR (1993) Polymer Preprints 34:926; Macromolecules (1994) 27: 4220
19. Dormidontova EE, Erukhimovich I Ya, Khokhlov AR (1994) Macromol Chem Theory Simul 3:661
20. Nyrkova IA, Khokhlov AR, Doi M (1993) Macromolecules 26:3601
21. Khokhlov AR, Erukhimovich I Ya (1993) Macromolecules 26:7195
22. Schmidt-Rohr K, Clauss J, Spiess HW (1992) Macromolecules 25:3273
23. Halary JL, Cheikh Larby FB, Oudin P, Monnerie L (1988) Makromol Chem 189:2117
24. Muller G, Stadler R, Schlick S (to be published)
25. Koningsveld L, Stockmayer WH, (1990) Macromol Chem Macromol Symp 39:1
26. Callister S, Keller A, Hikmet RM (1990) Macromol Chem Macromol Symp 39:19
27. Leibler L, Sekimoto K (1993) Macromolecules 26:6937
28. Loyd S (1959) Mathematical Puzzles Dover Publications, New York.
29. Fischer EW (1993) Physica A 201:183
30. Lifshitz IM (1968) Zh Eksp Ter Fiz (Sov Phys JETP) 55:2408
31. Lifshitz IM, Grosberg A Yu, Khokhlov AR (1978) Rev Mod Phys 50:683
32. Grosberg A Yu, Khokhlov AR (1989) Statistical Physics of Macromolecules. Nauka Publishers, Moscow
33. Landau LD, Lifshitz EM (1976) Statistical physics, part I. Nauka Publishers, Moscow
34. Fredrickson GH, Helfand E (1987) J Chem Phys 87:697
35. Mayes AM, Olvera de la Cruz M (1989) J Chem Phys 91:7228
36. Dobrynin AV, Erukhimovich I Ya (1993) Macromolecules 26:276
37. Nesterov A Ye, Lipatov Yu S (1987) Phase State of Polymer Solutions and Blends. Kiev, Naukova Dumka

Received April 5, 1994;
accepted June 15, 1994

Authors' address:

Prof. Alexei R. Khokholov
Physics Department
Moscow State University
117234 Moscow, Russia